AUTHOR(S):

TITLE:

YEAR:

Publisher citation:

OpenAIR citation:

Introduction

Positron emission tomography/computed tomography (PET/CT) with[18]F-flourodeoxyglucose (FDG) has a clear role in oncological applications with the fused images[1,2] providing improved detectability and lesion localisation accuracy.[3] Furthermore, the use of diagnostic quality CT with PET can offer advantages over standalone CT for accurate staging of disease due to a better assessment of nodal and metastatic involvement.[4] However, the benefits of these examinations need to be balanced against the lifetime attributable risk of cancer from a combined PET/CT investigation.[5]

Patient dose associated with PET/CT can be very high, and a high proportion of the dose is due to the diagnostic quality (DQ) CT examination. Recent technological improvements, notably time of flight (TOF),[6,7] have been implemented to enable the superior spatial resolution of modern PET/CT systems, and along with a strategy of calculating weight based injected activity[8–10] it has resulted in reduced radiation dose, with a preference to increase emission time rather than injected activity for obese patients.[6] Early reports of radiation dose in PET/CT, combining ^{18}F-FDG with DQ CT could produce effective dose in the range of 24-46 mSv.[5,11,12] However, a more recent Korean study reports an average radiation dose of 12.2 mSv, based on a mean injected activity of 5.11±1.19 MBq per Kg and CT scan for attenuation correction (AC).[10] This is in line with other studies using CT for AC only, where a dose of 8.5 mSv has been reported.[11] In other words, by not acquiring the DQ images one can reduce the dose by up to a factor of 3. Before this is done one needs to assess the loss of lesion detection performance associated with not acquiring DQ images.

The EANM provides guidelines for different CT scanning strategies in PET/CT[13] and the authors of the current study also recognise that funding and availability of contrast media may also dictate protocol, with variations in practice globally. In the UK, typical practice is for low-dose CT to be performed on all patients for AC. DQCT would only be required for a limited field of view over an area of clinically relevant interest if a standalone DQCT has not yet been completed. However, the evaluation of images suitable for CTAC can be difficult, with low positive predictive values reported in single photon emission computed tomography/computed tomography (SPECT/CT).[14] Nodule detection within the thorax has high clinical importance since a nodule can represent an early manifestation of lung cancer.[15] For small nodules, FDG-PET can be associated with false negatives,[15] thus giving more importance to the CT data for nodule detection. Evaluation of CTAC images remains a controversial issue, with variations in reporting practice down to local protocol and interpretations of IRMER regulation 7.8; '…ensure that a clinical evaluation of the outcome of each medical exposure is recorded'.[16]

A previous study[17] has assessed nodule detection performance in the CT images acquired for AC during SPECT/CT. This observer performance study compared nodule detection in the AC images produced by a range of CT acquisition parameters on systems from different manufacturers, revealing significant differences in nodule detection between SPECT/CT systems for images acquired for AC.[17] However, this study did not compare AC and DQ images for nodule detection on the same PET/CT system.

The purpose of our study is to compare the nodule detection performance provided by images acquired with diagnostic quality against those acquired with the primary purpose of AC.

Method

Image Acquisition

AC and DQ images were acquired on a GE Discovery 670 64-slice PET/CT system (*General Electric Healthcare, Waukesha, WI, USA*). CT images of the anthropomorphic chest phantom (*Lungman N1 Multipurpose Chest Phantom, Kyoto Kagaku Company Ltd, Japan*) were acquired for five different configurations of nodule position. For each configuration, the phantom was loaded with 12 nodules, measuring 5, 8, 10 and 12 mm diameters and contrasts -800, -630 and +100 HU. The size, HU and precise anatomical position of all nodules were recorded at the time of insertion. There were no duplicate nodules, i.e., nodules with same diameters and contrasts, in the same transaxial slice.

The CT images were acquired per the imaging protocol of our clinical partner, summarised in Table 1. AC and DQ images were acquired with automatic tube current modulation (ATCM). The CT component of this hybrid system uses a manufacturer termed "noise index" for automatic exposure control. The "noise index", referenced to the standard deviation of CT numbers in a water phantom measured on the CT scout (planning image), uses an algorithm to maintain levels of image noise as attenuation varies between projections.[18–20] The minimum and maximum tube current (mA) and "noise index" were set for AC and DQ acquisitions. Table 1 lists the remaining technical parameters used to acquire the AC and DQ images. Scan and reconstruction field of view (FOV) are protocol driven: to provide correction of photon attenuation (AC) and for image fusion (DQ). The remaining difference in acquisition parameters between AC and DQ images is the reconstructed slice thickness.

Dose length product (DLP) is reported by the CT scanner as an estimate of dose received; computed tomography dose index (CTDI) is not a robust measure of dose for evaluations using ATCM.[21]

Acquisition	kVp	Noise Index	Mean mA (min-max)	Recon. Slice (mm)	Pitch	Matrix Size	Scan FOV (mm)	Recon FOV (mm)	Pixel Size (mm)	DLP (mGy-cm)
AC	120	40.00	34.8±4.8 (30-42)	2.5	1.375	512x512	700	500	0.98	44.6
DQ	120	24.24	228.5±53.2 (143-292)	1.25	1.375	512x512	500	360	0.70	243.3

Table 1: The parameters used for image acquisition and reconstruction for both diagnostic quality (DQ) CT and CT for attenuation correction (AC). Noise index is the standard deviation of pixel values; this determines the mean tube current (mA) within a pre-determined range (max-min). FOV, field of view; Recon, reconstruction.

Observer Performance Study

A total of 45 normal cases (trans-axial slices with no simulated nodules) and 47 abnormal cases (transaxial slices) containing 1-3 simulated nodules (average 1.26 per abnormal case) were selected for the observer study from the AC and DQ image data. A case was defined as a single transaxial slice. A histogram illustrates the distribution and type of nodules used in this study, Figure 1. Image display and recording of interpretations were performed using ROCView[22] (*Bury St Edmunds, UK, www.rocview.net*) using a 22" widescreen monitor at 60Hz (*HP L2245wg, 1680x1050, 1.8 megapixels, Hewlett Packard, Palo Alto, CA, USA*) calibrated using X-Rite i1 and Eye-One Match 3 software (*X-Rite, Grand Rapids, MI, USA*). Observers were instructed to mark the centre of each nodule using a mouse click. A slider-bar rating scale (1-10) was used to rate confidence. An acceptance radius (AR), defined as the maximum distance, in order to be classified as a lesion localization, between the centre of a mark and the centre of the nearest nodule, was used to classify marks as lesion localization. This was set at 20-pixels.
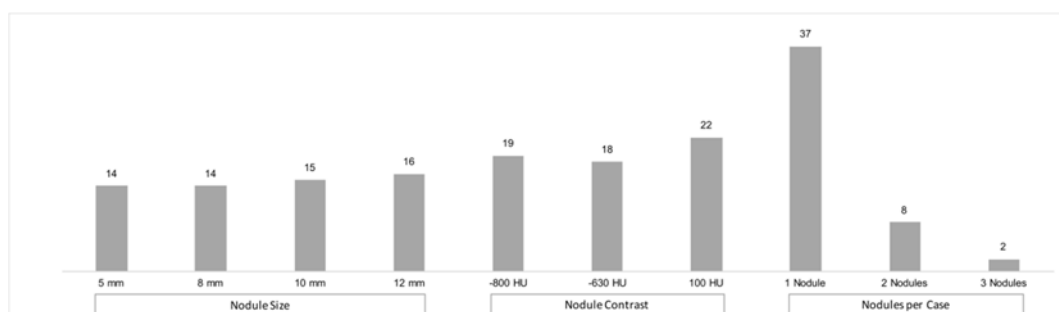

Figure 1: A histogram to explain the frequency and type of simulated nodules used in this study.

Cases were displayed in a different randomised order for each observer but on a fixed lung window (width 1500, level -500) for optimal evaluation of the simulated nodules. The observers comprised of 4 radiographers (5-16 years CT experience), 3 radiographers who provide diagnostic reports as part of their practice (2-14 years CT experience) and 2 nuclear medicine technologists (2-3 years CT experience). The nine observers were informed of the approximate 50:50 ratio of normal and abnormal cases and the range and characteristics of the nodules. Observers were also provided with a training dataset of ten images to familiarise themselves with the appearances of the phantom and nodules, and the procedure to mark and rate the nodules under the free-response paradigm using the user interface. These training requirements were deemed adequate since there was no need to manipulate images, while a phantom removes the influence of case variation. Additionally, the requirement for image randomisation and consideration of memory effect precautions, that are standard with clinical studies, are unnecessary with this phantom study.

Statistical Analysis

Since the observer task required the localisation of nodules we desired an analysis method that accounts for localisation. The ROC paradigm considers only a single rating for the entire case, thus ignoring the location of the nodules. The equally weighted jackknife alternative FROC JAFROC (wJAFROC) figure of merit[23], which accounts for location information, is the weighted empirical probability that a lesion is rated higher than any mark on a normal case. In addition to this, the area under the empirical highest rating inferred ROC curve was also used as a figure of merit. A random reader fixed case analysis was performed to test for a statistical difference in nodule detection performance. Case was regarded as a fixed factor because case variability does not apply to when using a single phantom; of course, the results are then specific to the phantom used.

Data were analysed using an R[24] package implemented JAFROC analysis, available at (*https://cran.r-project.org/web/packages/RJafroc/index.html*). Two situations were analysed: (i) wJAFROC; and (ii) a highest-rating inferred ROC analysis (HR inferred ROC) that was derived from FROC data. A difference in nodule detection performance was considered statistically significant when the p-value of the overall F-test was less than 0.05, or equivalently, the 95% confidence interval for the treatment pairing did not include zero. To control the probability of Type I error test alpha was set at 0.05.

Results

Nodule detection as measured by either FOM was significantly better on the diagnostic quality images. The relevant statistics, P values, treatment difference and FOMs, including 95% confidence intervals (CI) are summarised in Table 2, which lists the wJAFROC analysis and the HR inferred ROC analysis. The FOM differences in Table 2 are negative since AC is treated as the first modality in the analysis, and the FOM for AC was smaller than that for DQ. We also analysed the data in terms of lesion level detection (sensitivity) using the maxLLF (maximum lesion localisation fraction) FOM in Rjafroc. Again, a statistically significant difference was found in favour of DQ ($F(1,8) = 56.25$, $p = 0.0001$); DQ FOM 0.857(0.779,0.935), AC FOM 0.751(0.673,0.830). Typical images for DQ and AC are shown in Figure 2a & 2b.

Analysis	F-Statistic	P value	FOM Difference (95% CI)	Figure of Merit (95% CI)	
				AC	DQ
wJAFROC	$F(1,8) = 24.18$	0.0012	-0.07 (-0.11,-0.04)	0.776 (0.693,0.858)	0.849 (0.789,0.910)
HR Inferred ROC	$F(1,8) = 10.13$	0.0129	-0.05 (-0.09,-0.01)	0.847 (0.787,0.907)	0.899 (0.862,0.936)

Table 2: The wJAFROC and highest rating inferred ROC statistics, figures of merit and inter-treatment difference with 95% confidence intervals (CI). Both analyses were sensitive enough to find a statistical difference in nodule detection performance, where the P value was less than 0.05 and the 95% CI of the treatment difference did not include zero.
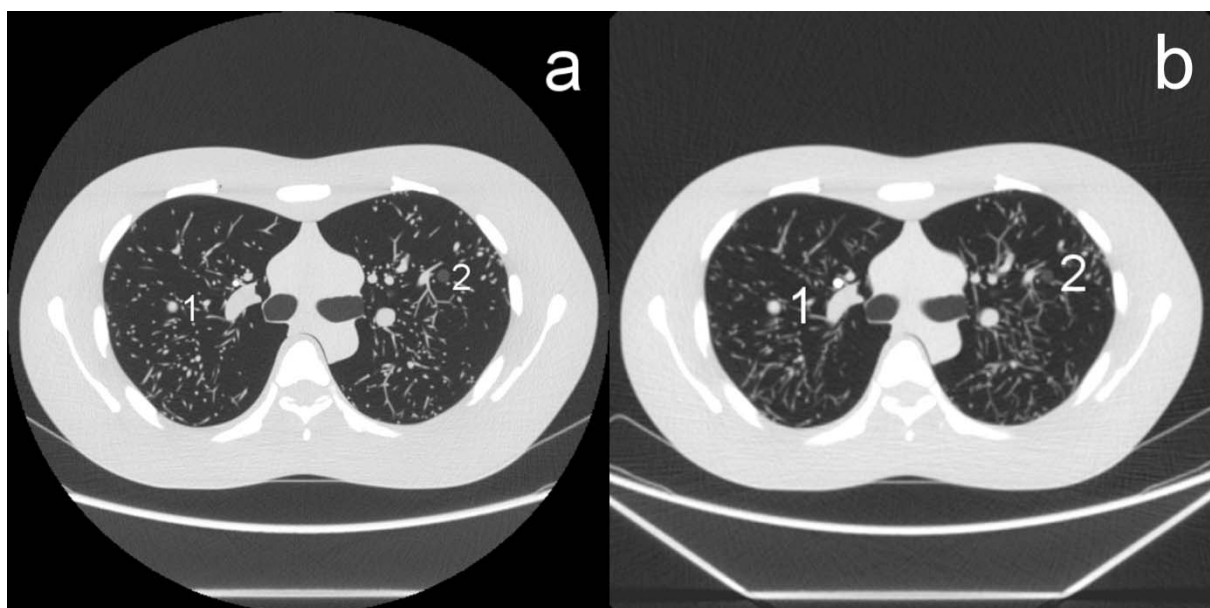

Figure 2: An example of the images produced with DQ (a) and AC (b). This case shows two nodules labelled 1 (right simulated lung, 10 mm 100 HU nodule) and 2 (left simulated lung, 8 mm -800 HU nodule).

The wJAFROC analysis showed a notable increase in statistical significance over the HR inferred ROC analysis, where the ROC analysis produced the expected inflation in figure of merit with a smaller treatment difference, Table 2. An inflated FOM is evident with the inferred ROC analysis since the wJAFROC FOM uses only the correctly localised lesions; the occasions where a non-lesion localisation (NL) rating exceeds the lesion localisation (LL) rating are not included. The ROC FOM does include these ratings, as it is not sensitive to location data; as a result the fraction of cases where a diseased case is rated higher than a non-diseased case is increased. A larger difference between DQ and AC is seen with wJAFROC as it is measured over a larger range (0 to 1, wAFROC; 0.5 to 1, ROC).

Despite the lower statistical significance of the HR inferred ROC analysis it is important to note that the difference between the two treatments (AC and DQ) was large enough for a statistical difference to be observed even with ROC analysis. Observer averaged empirical wAFROC plots and the corresponding highest-rating inferred ROC plots for DQ and AC images are displayed in Figure 3.

To analyse the impact of mAs and slice thickness, and thus determine the controlling factor on nodule detection, we eliminated the smallest nodules (5 mm) from supplementary analyses. We hypothesised that if a statistically significant difference remained between CTAC and DQCT then it is more likely that tube charge (mAs) is the controlling factor, rather than slice thickness. We again performed wJAFROC and HR inferred ROC analysis, Table 3. For the sub-evaluation it is necessary to apply a Bonferroni correction to account for multiple comparisons. The corrected value of alpha is 0.05/2 (or 0.025).

Supplementary Analysis	F-Statistic	*P* value	FOM Difference (95% CI)	Figure of Merit (95% CI)	
				AC	DQ
wJAFROC	F(1,8) = 8.60	0.0189	-0.04 (-0.07,-0.01)	0.829 (0.760,0.898)	0.868 (0.817,0.918)
HR Inferred ROC	F(1,8) = 4.95	0.0568	-0.03 (-0.06,0.00)	0.890 (0.839,0.941)	0.920 (0.888,0.951)

Table 3: Results of supplementary analyses with 5 mm nodules removed from the dataset, showing the wJAFROC and highest rating inferred ROC statistics, figures of merit and inter-treatment difference with 95% confidence intervals (CI). Only the wJAFROC method was sensitive enough to show a significant difference between AC and DQ.

Even with removal of the 5 mm nodules the wAFROC analysis shows a significant difference between DQ and AC (p-value lower than the Bonferroni corrected value of alpha), suggesting that the main contributor to the difference is the large difference in mAs - which

implies more noise in the AC images - which would impact on detectability of low contrast large nodules. This would suggest that the controlling influence on nodule detection was tube charge (mAs) for the nodules and phantom reported in this study, since removal of the smaller nodules, most likely to be affected by slice thickness, did not change the overall outcome. This supplementary analysis adds weight to the additional value of location based analysis methods in observer studies, where the HR inferred ROC analysis was not sensitive to this result.

Analysis of nodule detection rates between AC and DQ showed that differences existed for most nodule types of size and contrast. However, the detection difference was largest for 5mm nodules with 93 successful localisations on DQ images and 64 successful localisations on AC images.
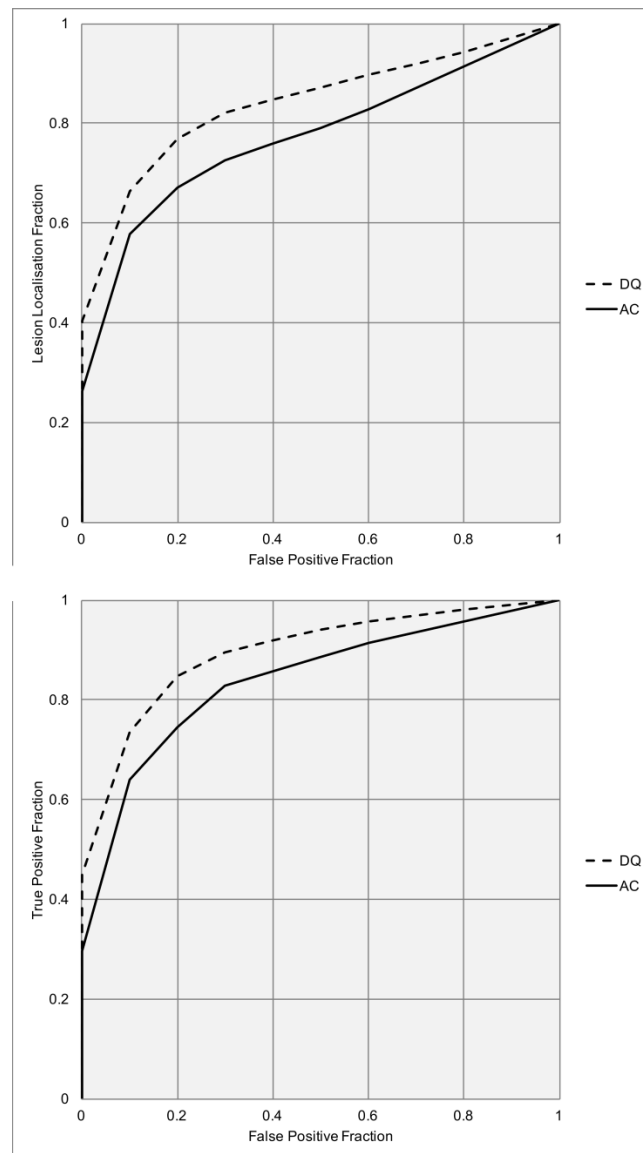

Figure 3: The empirical reader-averaged wAFROC plot and the corresponding highest-rating inferred ROC plot.

Discussion

This study found nodule detection to be significantly poorer on images acquired for AC compared to DQ. Based on these results we do not advocate acquiring only AC images if nodule detection in the size range quoted in this study is required. The limited usefulness of the AC images for nodule detection may have implications for PET/CT protocols that use AC only, if the focus of the examination is pulmonary nodules.

A supplementary analysis, excluding the smallest nodule size (5 mm), still generated a statistically significant result. This is suggestive of tube charge (mAs) being the controlling factor in this work, rather than slice thickness. In this study the average mAs, as controlled by ATCM, for the DQ images was much higher at 228.5±53.2 (range 143-292) compared to 34.8±4.8 (range 30-42) for the AC images. This effect of mAs seems to be confirmed by other recent work.[25] However, the potential impact of spatial resolution should not be ignored, since smaller slice thickness can result in higher nodule contrast due to decreased partial volume effects. Pixel size will also be reduced in AC image; this loss of resolution can be unavoidable since a larger field of view is required to minimise truncation artefacts.[26]

Several authors[12,27,28] have considered dose optimisation in PET/CT using subjective evaluations to compare image quality of AC acquisitions. None of the previous works evaluating radiation dose in PET/CT reported observer performance studies. The limitations of objective and subjective evaluations are often overlooked in evaluations of technology. However, these studies suggest agreement with the current study, finding low-dose CT not to be equivalent to DQ CT. A clinical evaluation of the AC image in SPECT/CT has come to our attention during the writing of this work. Coward et al[14] reviewed the AC images in 3485 patients attending for myocardial perfusion imaging; they found a positive predictive value of only 12% for incidental findings revealed in the AC image, suggesting that routine reporting of these images was not beneficial. This would appear to confirm the findings of our study.

It is important to note that lesion detection in clinical PET/CT is not reliant only on CT imaging. The metabolism of a lesion is also important in PET/CT; a small lesion that is metabolically active is likely to be seen on PET even if the morphological characteristics of the lesion prevent it from being picked up on CT. The converse may also be true, where a larger less active, or non-avid lesion, may be overlooked. Well differentiated thyroid carcinomas tend to have lower FDG avidity while lung carcinoids are typically considered non-avid.[29] Hybrid imaging improves the detection of non-FDG avid tumours and lesions but questions remain about how much time should be invested assessing AC images for non-avid abnormalities.

An additional point of interest concerns our secondary analysis of data to investigate the impact of tube charge and slice thickness. This analysis highlights the statistical power advantage of a location based analysis in observer studies. The wJAFROC FOM was still able to detect a statistical difference in nodule detection performance when the smallest nodules (5 mm) were removed, while the HR ROC analysis was not sensitive to the difference in performance. This is an important point to consider when planning an observer study that involves precise localisation. We also applied the maxLLF FOM to indicate lesion level detection (sensitivity); this again showed a highly significant difference in performance in favour of DQ.

There are some limitations to our work. Phantom studies are useful when comparing imaging methods under controlled conditions, removing the influence of case variation. However, the relevance to clinical interpretations can be limited and of this type of result should be carefully considered. Additionally, this phantom did not account for respiratory motion. Continuous breathing techniques have been employed in PET/CT examinations but there is a growing acceptance of breath-hold CT scanning[30–32] for pulmonary pathology, which is better represented by the phantom model in this research than a simulation of respiratory motion. However, respiratory motion is an important consideration, but currently we do not know the impact of respiratory motion on nodule detection in this phantom. A study that emulates respiratory motion in this phantom is underway.

Additionally, we do not know the impact of ATCM on nodule detection. ATCM is widely accepted as a suitable dose reduction method for DQ imaging[33–37] but despite the mA being limited to operate within upper and lower limits,[35] previous work[19] suggests the selection of "noise index" can be arbitrary and radiation dose may not be adequately optimised. Future work could assess nodule detection in DQ images acquired with and without ATCM using observer performance studies patterned on the current work.

Conclusion

Nodule detection was significantly worse on images acquired for AC as compared to DQ and it suggests that images for AC should not be used for interpretation of non-avid lesions. Even when the smallest nodules (5 mm) were removed from the analysis, a statistically significant difference remained for the specification of nodules used in this study.

References

1.   Beyer T, Townsend DW, Brun T, et al. A combined PET/CT scanner for clinical oncology. *J Nucl Med*. 2000;41(8):1369-1379. http://www.ncbi.nlm.nih.gov/pubmed/10945530.

2.   Townsend DW, Beyer T. A combined PET/CT scanner: The path to true image fusion. In: *British Journal of Radiology*. Vol 75. ; 2002.

3.   Ay MR, Zaidi H. Assessment of errors caused by X-ray scatter and use of contrast medium when using CT-based attenuation correction in PET. *Eur J Nucl Med Mol Imaging*. 2006;33(11):1301-1313. doi:10.1007/s00259-006-0086-6.

4.   Antoch G, Freudenberg LS, Beyer T, Bockisch A, Debatin JF. To enhance or not to enhance? 18F-FDG and CT contrast agents in dual-modality 18F-FDG PET/CT. *J Nucl Med*. 2004;45 Suppl 1:56S-65S.

5.   Huang B, Law MW-M, Khong P-L. Whole-body PET/CT scanning: estimation of radiation dose and cancer risk. *Radiology*. 2009;251(1):166-174. doi:10.1148/radiol.2511081300.

6.   Beyer T, Czernin J, Freudenberg LS. Variations in Clinical PET/CT Operations: Results of an International Survey of Active PET/CT Users. *J Nucl Med*. 2011;52(2):303-310. doi:10.2967/jnumed.110.079624.

7.   Karakatsanis NA, Fokou E, Tsoumpas C. Dosage optimization in positron emission tomography: state-of-the-art methods and future prospects. *Am J Nucl Med Mol Imaging*. 2015;5(5):527-547. www.ajnmmi.us.

8.   Geismar JH, Stolzmann P, Sah B-R, et al. Intra-individual comparison of PET/CT with different body weight-adapted FDG dosage regimens. *Acta Radiol Open*. 2015;4(2):1-9. doi:10.1177/2047981614560076.

9.   Sanchez-Jurado R, Devis M, Sanz R, Aguilar JE, Puig Cozar M d., Ferrer-Rebolleda J. Whole-Body PET/CT Studies with Lowered 18F-FDG Doses: The Influence of Body Mass Index in Dose Reduction. *J Nucl Med Technol*. 2014;42(1):62-67. doi:10.2967/jnmt.113.130393.

10.   Kwon HW, Kim JP, Lee HJ, et al. Radiation dose from whole-body F-18 fluorodeoxyglucose positron emission tomography/computed tomography: Nationwide survey in Korea. *J Korean Med Sci*. 2016;31:69-74. doi:10.3346/jkms.2016.31.S1.S69.

11.   Brix G, Lechel U, Glatting G, et al. Radiation exposure of patients undergoing whole-

body dual-modality 18F-FDG PET/CT examinations. *J Nucl Med*. 2005;46(4):608-613. doi:46/4/608 [pii].

12. Tonkopi E, Ross AA, MacDonald A. CT dose optimization for whole-body PET/CT examinations. *Am J Roentgenol*. 2013;201(2):257-263. doi:10.2214/AJR.12.10495.

13. Boellaard R, Delgado-Bolton R, Oyen WJG, et al. FDG PET/CT: EANM procedure guidelines for tumour imaging: version 2.0. *Eur J Nucl Med Mol Imaging*. 2014;42(2):328-354. doi:10.1007/s00259-014-2961-x.

14. Coward J, Lawson R, Kane T, et al. Multicentre analysis of incidental findings on low-resolution CT attenuation correction images: an extended study. *Br J Radiol*. 2015;88(1056):20150555. doi:10.1259/bjr.20150555.

15. Brandman S, Ko JP. Pulmonary nodule detection, characterization, and management with multidetector computed tomography. *J Thorac Imaging*. 2011;26(2):90-105. doi:10.1097/RTI.0b013e31821639a9.

16. Department of Health. *The Ionising Radiation (Medical Exposure) Regulations 2000*. United Kingdom; 2000:1-12. http://www.legislation.gov.uk/uksi/2000/1059/contents/made.

17. Thompson JD, Hogg P, Manning DJ, Szczepura K, Chakraborty DP. A Free-response Evaluation Determining Value in the Computed Tomography Attenuation Correction Image for Revealing Pulmonary Incidental Findings. *Acad Radiol*. 2014;21(4):538-545. doi:10.1016/j.acra.2014.01.003.

18. McCollough CH, Bruesewitz MR, Kofler JM. CT dose reduction and dose management tools: overview of available options. *Radiographics*. 2006;26(2):503-512. doi:10.1148/rg.262055138.

19. Jackson J, Pan T, Tonkopi E, Swanston N, Macapinlac HA, Rohren EM. Implementation of automated tube current modulation in PET/CT: prospective selection of a noise index and retrospective patient analysis to ensure image quality. *J Nucl Med Technol*. 2011;39(2):83-90. doi:10.2967/jnmt.110.075283.

20. McCollough C, Primak N. A, Braun N, Kofler J, Yu L, Cristner J. Strategies for Reducing Radiation Dose. *Radiol Clin North*. 2009;47(1):27-40. doi:10.1016/j.rcl.2008.10.006.Strategies.

21. Dixon RL, Boone JM. Dose equations for tube current modulation in CT scanning and the interpretation of the associated CTDIvol. *Med Phys*. 2013;40(11):111920. doi:10.1118/1.4824918.

22. Thompson JD, Hogg P, Thompson S, Manning DJ, Szczepura K. ROCView: prototype software for data collection in jackknife alternative free-response receiver operating characteristic analysis. *Br J Radiol.* 2012;85(1017):1320-1326. doi:10.1259/bjr/99497945.

23. Chakraborty DP, Berbaum KS. Observer studies involving detection and localization: Modeling, analysis, and validation. *Med Phys.* 2004;31(8):2313-2330. doi:10.1118/1.1769352.

24. R Core Team. R: A language and environment for statistical computing. *R Found Stat Comput.* 2015:http://www.r-project.org/. http://www.r-project.org/.

25. Thompson JD, Chakraborty DP, Szczepura K, et al. Effect of reconstruction methods and x-ray tube current–time product on nodule detection in an anthropomorphic thorax phantom: A crossed-modality JAFROC observer study. *Med Phys.* 2016;43(3):1265-1274. doi:10.1118/1.4941017.

26. Sureshbabu W, Mawlawi O. PET/CT Imaging Artifacts. *J Nucl Med Technol.* 2005;33(3):156-161. http://tech.snmjournals.org/content/33/3/156.figures-only.

27. Kumar S, Pandey AK, Sharma P, Malhotra A, Kumar R. Optimization of the CT acquisition protocol to reduce patient dose without compromising the diagnostic quality for PET-CT. *Nucl Med Commun.* 2012;33(2):164-170. doi:10.1097/MNM.0b013e32834e0993.

28. Gollub MJ, Hong R, Sarasohn DM, Akhurst T. Limitations of CT during PET/CT. *J Nucl Med.* 2007;48(10):1583-1591. doi:10.2967/jnumed.107.043109.

29. Takalkar A, El-Haddad G, Lilien D. FDG-PET and PET/CT - Part II. *Indian J Radiol Imaging.* 2008;18(1):17. doi:10.4103/0971-3026.38504.

30. Meirelles GSP, Erdi YE, Nehmeh SA, et al. Deep-inspiration breath-hold PET/CT: clinical findings with a new technique for detection and characterization of thoracic lesions. *J Nucl Med.* 2007;48(5):712-719. doi:10.2967/jnumed.106.038034.

31. Yamaguchi T, Ueda O, Hara H, et al. Usefulness of a breath-holding acquisition method in PET/CT for pulmonary lesions. *Ann Nucl Med.* 2009;23(1):65-71. doi:10.1007/s12149-008-0206-4.

32. Mitsumoto K, Abe K, Sakaguchi Y, et al. Determination of the optimal acquisition protocol of breath-hold PET/CT for the diagnosis of thoracic lesions. *Nucl Med Commun.* 2011;32(12):1148-1154. doi:10.1097/MNM.0b013e32834bbda7.

33. Kalra MK, Maher MM, Toth TL, et al. Techniques and applications of automatic tube

current modulation for CT. *Radiology*. 2004;233(3):649-657. doi:10.1148/radiol.2333031150.

34.   Schindera ST, Nelson RC, Yoshizumi T, et al. Effect of Automatic Tube Current Modulation on Radiation Dose and Image Quality for Low Tube Voltage Multidetector Row CT Angiography. Phantom Study. *Acad Radiol*. 2009;16(8):997-1002. doi:10.1016/j.acra.2009.02.021.

35.   Iball GR, Tout D. Computed tomography automatic exposure control techniques in 18F-FDG oncology PET-CT scanning. *Nucl Med Commun*. 2014;35(4):372-381. doi:10.1097/MNM.0000000000000064.

36.   Costello JE, Cecava ND, Tucker JE, Bau JL. CT radiation dose: current controversies and dose reduction strategies. *Am J Roentgenol*. 2013;201(6):1283-1290. doi:10.2214/AJR.12.9720.

37.   Kaza RK, Platt JF, Goodsitt MM, et al. Emerging techniques for dose optimization in abdominal CT. *Radiographics*. 2014;34(1):4-17. doi:10.1148/rg.341135038.